Theoretical study of the H + Br_2 and Mu + Br_2 reactions: A new ab initio potential energy surface and quantum dynamics calculations

Toshiyuki Takayanagi

Department of Chemistry, Saitama University, 255 Shimo-Okubo, Sakura-ku, Saitama City, Saitama 338-8570, Japan

Abstract

A new global potential energy surface for the H + Br_2 → HBr + Br reaction has been developed at the MRCI+Q/ang-cc-pVTZ ab initio level of theory. It has been found that this level calculation gives a negative barrier slightly below the H + Br_2 reactant energy level. Time-dependent and time-independent quantum dynamics calculations have been performed on this potential energy surface. The calculated cumulative reaction probabilities for $J = 0$ around the reaction threshold energy region show a very similar behavior for both the H + Br_2 and Mu + Br_2 reaction, in qualitative disagreement with experimental measurements, where a positive activation energy was observed for the H + Br_2 reaction while a negative activation energy for the Mu + Br_2 reaction. Variational calculations of vibrational energy levels have also been performed to study dynamical vibrational bonding for the Br-Mu-Br molecule. It has been found that the system has several vibrational bonding states, whose wave functions are localized around the transition-state of the Br + MuBr' → MuBr + Br' exchange reaction, below the lowest Br + MuBr asymptotic energy level. This result qualitatively supports the recent experimental finding that a long-lived radical containing a Mu atom is produced in the Mu + Br_2 reaction.

E-mail: tako@chem.saitama-u.ac.jp

1. Introduction

The reaction of hydrogen atoms with diatomic halogen molecules (F_2, Cl_2 and Br_2) in the gas phase is one of the prototypical atom-diatom reactions and has been extensively studied from both experimental and theoretical sides [1-12]. However, previous rate constant measurement studies for the H + Br_2 reaction and its isotopic variants show a quite strange behavior that has not been observed in the corresponding F_2 and Cl_2 reactions. Wada et al. [2] have measured thermal rate constants for the H + Br_2 and D + Br_2 reactions using a pulse radiolysis-resonance absorption technique in the temperature range of 214-295 K and observed a positive activation energy of about 1.4 kcal/mol from Arrhenius plots of the measured rate constants. On the other hand, Gonzalez et al. [1] have measured thermal rate constants of the Mu + Br_2 reaction, where Mu (muonium) is a light isotope of hydrogen with its mass being 1/9 of that of H, using a muon-spin-rotation (μSR) technique. They have found that the measured rate constant decreases as the temperature of the system increases over the range of 200-400 K. Thus, the Mu + Br_2 experiment exhibits an apparent negative activation energy behavior. The observed negative barrier behavior is in qualitative agreement with early molecular beam studies [13, 14] for the H(D) + Br_2 reaction rather than the kinetic study of Wada et al [2]. Interestingly, Gonzalez et al. [1] have suggested that either a pronounced steric effect or the formation of a long-lived $MuBr_2$ radical could account for the observed negative activation behavior.

Very recently, Ghandi et al. [15] have reported preliminary experimental data for the evidence of a free radical containing a Mu atom produced from the Mu + Br_2 reaction. They have tentatively assigned the observed radical as the unconventional Br-Mu-Br dynamical binding molecule since it has previously been pointed out, from quantum scattering calculations, that Heavy-Light-Heavy (HLH) reaction systems can sometimes lead to the formation of unconventional dynamical bonds called "vibrational bonds" [16-18]. The vibrational bonds are formed when two heavy atoms are bound together by vibration of a light central atom, even if the potential energy surface for the H + LH $\rightarrow$ HL + H reaction is purely repulsive. In fact, Clary and Connor [17, 18]

have carried out systematic three-dimensional quantum variational calculations for the Br-X-Br system with X = H, D and Mu on a less accurate semiempirical potential energy surface and theoretically confirmed the existence of vibrational bonding molecules. It should be emphasized that these theoretical studies significantly stimulated experimental studies on the detection of vibrational bonding molecules by measuring the photodetachment spectra of the $(Y\text{-}X\text{-}Y)^-$ anions with Y = Cl, Br and I [19].

Motivated by the current status on the reaction dynamics of the H + Br_2 reaction and its isotopic variants as mentioned above, we have just started a research project for these reactions from a theoretical point of view. As far as we are aware, there has been no report on the global ab initio potential energy surface for the H + Br_2 reaction system. Here, we firstly develop a new ab initio potential energy surface and report some preliminary quantum dynamics calculations on the newly developed potential energy surface.

2. Ab initio electronic structure calculations of the potential energy surface

In order to determine the appropriate ab initio level of theory for obtaining a global potential energy surface, we have firstly calculated minimum-energy potential profiles at two electronic structure levels. We have employed a spin-restricted coupled cluster method with single, double, and noniterative triple excitations [RCCSD(T)] and a multi-reference configuration interaction (MRCI) method with single and double excitations. The Davidson correction (+Q) [20, 21] was added to the obtained MRCI energies. Two basis sets were employed: aug-cc-pVTZ and aug-cc-pVQZ [22, 23]. In the MRCI+Q calculations, the molecular orbitals were determined for the lowest three doublet states using the state-averaged complete-active-space self-consistent-field (CASSCF) [24, 25]. The active space in the CASSCF calculations includes all 15 valence electrons and 9 valence orbitals. The spin-orbit interaction was completely ignored in this study. All ab initio electronic structure calculations were carried out

using the MOLPRO program package [26].

Fig. 1 displays potential energy profiles calculated at the RCCSD(T)/aug-cc-pVTZ, RCCSD(T)/aug-cc-pVQZ, MRCI+Q/aug-cc-pVTZ and MRCI+Q/aug-cc-pVQZ levels of theory as a function of the H-Br distance, where the Br-Br distance was optimized with respect to energy. Notice that only collinear configurations were considered since we have found that the collinear approach of the H atom to Br_2 is energetically most favorable. It is seen that the RCCSD(T)/aug-cc-pVTZ and RCCSD(T)/aug-cc-pVQZ level calculations give positive classical barriers higher than the asymptotic H + Br_2 potential bottom. The RCCSD(T)/aug-cc-pVTZ level calculations give a barrier height of 0.17 kcal/mol, while the RCCSD(T)/aug-cc-pVQZ level yields a somewhat lower barrier height of 0.07 kcal/mol. On the other hand, the MRCI+Q level calculations give negative barriers lower than the asymptotic H + Br_2 energy level for the two basis sets employed. In addition, it is found that the MRCI+Q/aug-cc-pVTZ and MRCI+Q/aug-cc-pVQZ methods give a very similar potential energy profile. It is also interesting to note that there exists a van der Waals well just before the abstraction barrier around R(H-Br) ~ 3 Å. The MRCI+Q calculations give somewhat deeper wells (~ 0.45 kcal/mol) than the RCCSD(T) results (~ 0.38 kcal/mol).

Since we have found that the MRCI+Q/aug-cc-pVTZ and MRCI+Q/aug-cc-pVQZ methods give a very similar potential energy profile, we have decided to employ the MRCI+Q/aug-cc-pVTZ level of theory for obtaining a global potential energy surface for the ^{2}A' ground state of the H + Br_2 reaction system in order to save computational time. All calculations were performed in C_s symmetry. Potential energies were calculated at the grid points defined by H-Br-Br internal coordinates, $r_{H\text{-}Br}$, $r_{Br\text{-}Br}$ and ∠H-Br-Br, where $r_{H\text{-}Br}$ is the distance between H and Br atoms and $r_{Br\text{-}Br}$ is the distance between two Br atoms. We have chosen 41 points for $r_{H\text{-}Br}$ in the range of 1-5 Å, 13 points for $r_{Br\text{-}Br}$ in the range of 2-3 Å and 9 points for the ∠H-Br-Br angle in the range of 20-180 degrees. A similar calculation was also performed with the Br-H-Br internal coordinates, $r_{H\text{-}Br}$, $r_{H\text{-}Br'}$ and ∠Br-H-Br, in order to describe the Br + HBr' → HBr + Br' exchange reaction region. We have chosen 41

points for $r_{H\text{-}Br}$ in the range of 1-5 Å, 8 points for $r_{H\text{-}Br'}$ in the range of 1-2 Å and 8 points for the ∠Br-H- Br angle in the range of 40-180 degrees. These sets of grids thus give about 7500 symmetry unique points. Finally, a three-dimensional cubic spline interpolation was employed to yield a global potential energy surface. Before presenting details of the calculated potential energy surface, it is informative to give the accuracy of the present MRCI+Q/aug-cc-pVTZ level calculations. The dissociation energy of Br_2 was calculated to be 2.02 eV while the corresponding experimental value is reported to be 1.99 eV. Also, the exothermicity of the H + Br_2 → HBr + Br reaction was calculated to be 1.88 eV, which is somewhat smaller than the experimental exothermicity (1.92 eV). Thus, the present ab initio calculations have an error of about 0.04 eV; however, it should be again noted that the present electronic structure calculations do not include spin-orbit interaction at all.

Fig. 2 displays two-dimensional contour plots of the calculated potential energy surface in the entrance region of the H + Br_2 reaction. The contour increment is 0.1 eV and the contour energies are given relative to the asymptotic H + Br_2 potential bottom. We can see that there is no positive barrier for the H + Br_2 → HBr + Br reaction in the ∠H-Br-Br angle range of 160-180 degrees. On the other hand, there is a substantial barrier for non-collinear approaches for ∠H-Br-Br < 160 degree. Thus, nearly collinear approaches are energetically favorable for the H + Br_2 → HBr + Br reaction.

Fig. 3 shows two-dimensional contour plots of the potential energy surface for the Br + HBr' → HBr' + Br exchange reaction as a function of the two H-Br distances. Notice that these contour plots are symmetric with respect to the R(H-Br) = R(H-Br') line. Plot conventions are exactly the same as Fig. 2. Unlike the H + Br_2 → HBr + Br reaction, it can be seen that the non-collinear approach with ∠Br-H-Br ~ 140 degrees gives the lowest barrier of about 0.3 eV. This trend is quite similar to the Cl + HCl' → HCl' + Cl exchange reaction. Previous theoretical study by Schatz and co-workers [27] shows that a saddle point (~ 0.37 eV above the reactants) occurs on the $1^2A'$ ground state potential energy surface at the ∠Cl-H-Cl' internal bond angle of 137.4°. However, it should be emphasized that the inclusion of spin-orbit interaction may significantly affect the features of the potential energy surface for the Br + HBr' → HBr' + Br

exchange reaction due to the large spin-orbit interaction in the Br(^2P) atom. Thus, sophisticated nonadiabatic multi-surface treatments [27, 28] should be needed to describe this region more quantitatively.

3. Quantum dynamics calculations

Using the newly developed potential energy surface, we have carried out quantum dynamics calculations to obtain cumulative reaction probabilities for the H + Br_2 and Mu + Br_2 reactions since the cumulative reaction probability is most fundamental quantity for determining thermal rate constants. However, our calculations are limited to $J = 0$, where J is the total angular momentum quantum number because $J > 0$ calculations were prohibitively time-consuming due to the huge number of ro-vibrational states of the heavy Br_2 molecule. In spite of this limitation, we believe that the $J = 0$ quantum dynamics calculation is a good starting point for further theoretical developments. We have employed a closed-coupled, time-independent quantum reactive scattering method. The calculations were mostly carried out using the ABC code of Skouteris et al. [29] but a part of the calculations were performed with our own code [30] based on the adiabatically adjusting, principal axes hyperspherical (APH) approach developed by Pack and Parker [31]. Numerical parameters were carefully chosen to obtain fully converged computational results.

Fig. 4 shows the calculated cumulative reaction probabilities as a function of the total energy for the H + $Br_2 \rightarrow$ HBr + Br and Mu + $Br_2 \rightarrow$ MuBr + Br reactions. Here, the total energy is measured from the potential bottom of the H(Mu)+ Br_2 reactants. It is seen that the calculated cumulative reaction probabilities show a typical behavior although many sharp resonance peaks can be seen. These sharp resonances are presumably due to quasi-bound states trapped in the entrance H···Br_2 van der Waals well; however, notice that the energy resolution employed in the present calculations was not small enough to resolve all sharp resonance structures. It is also found that the absolute value of the cumulative reaction probability for the H + Br_2 reaction is larger

than that for Mu + Br_2 by a factor of about 4, suggesting a difference in the number of states around the reaction bottleneck or saddle point between these two reactions.

The most important point for determining the temperature dependence of thermal rate constants is a threshold behavior of the cumulative reaction probability. From the result presented in Fig. 4, it is found that the cumulative reaction probabilities for both H + Br_2 and Mu + Br_2 reactions quite suddenly increase just after the reaction threshold energy, which is defined as the energy level of the H + Br_2(v = 0, j = 0) reactants, where v and j are vibrational and rotational quantum numbers, respectively. This is a general behavior for chemical reactions without barriers or with extremely low barriers. Thus, this is an expected result since the potential energy surface developed in this study does not have a positive barrier, as mentioned in the previous section. In order to understand the threshold behavior of the cumulative reaction probability more quantitatively, we also show expansions of the probabilities around the reaction threshold region in Fig. 4 as insets. It is interesting to note that the reaction probabilities show a typical behavior for reactions with barriers; however, the corresponding barrier height is estimated to be extremely small (~ 0.001 eV). This value would presumably be much smaller than the accuracy of the present ab initio electronic structure calculations. Another important point which should be mentioned is that the threshold behavior of the cumulative reaction probability is quite similar for both H + Br_2 and Mu + Br_2 reactions. This result qualitatively disagrees with the previous experimental studies. As mentioned in Introduction, previous experimental measurements of thermal rate constants showed very different temperature dependence between H + Br_2 and Mu + Br_2 reactions: a positive activation energy for H + Br_2 while a negative activation energy for Mu + Br_2. Thus, this experimental finding cannot probably be explained by the present quantum dynamics calculations on the new potential energy surface although the present quantum dynamics calculations are restricted only to J = 0. Further quantum dynamics calculations for J > 0 would definitely be necessary to understand this disagreement. Theoretical calculations employing the centrifugal-sudden approximation are currently underway in our laboratory.

Next, let us consider the effect of the entrance H···Br_2 van der Waals well on the reaction dynamics in somewhat more detail. As shown previously, the present H-Br-Br potential energy surface has a relatively deep van der Waals well (~ 0.4 kcal/mol) in the entrance region. This suggests that there exist some bound states below the lowest H(Mu) + Br_2(v = j = 0) reactant energy level. Of course, these states cannot be true bound states since these states can decay into the HBr + Br reaction products through quantum mechanical tunneling. This process is schematically shown in Fig. 5. If the lifetime of such a resonance is long, the following three-body process may also contribute to the overall reaction rate:

$$H + Br_2(v = 0, j = 0) + M \rightleftarrows H\cdots Br_2 + M \quad (1)$$

$$H\cdots Br_2 \rightarrow HBr + Br \quad (2)$$

Here, M is the third-body that can carry away the excess energy and H···Br_2 represents the van der Waals resonance state which occurs below the lowest H + Br_2(v = 0, j = 0) energy level. Note that these resonance states can decay only to reaction products via quantum tunneling.

In order to understand whether van der Waals resonance states do exist or not on the HBrBr (MuBrBr) potential energy surface, we have further carried out time-dependent quantum wave packet calculations. The reaction system was described by the standard J = 0 Hamiltonian expressed in Jacobi coordinates. The wave function was represented on a spatial grid in the radial coordinates (R, r) and in a Legendre basis for the angular coordinate γ. We have put an appropriate Gaussian wave function around the entrance van der Waals region and the wave packet was then propagated using a well-known split-operator method for time-evolution. The R and r contributions to the kinetic energy were evaluated using the standard fast-Fourier-transform algorithm, while the discrete-variable-representation (DVR) [32] scheme was used for γ. In order to avoid unphysical reflection of the wave packet at the edge of the grid, numerically optimized complex absorbing potentials were used over the last 25 % of the grids in R and r. Details of our wave packet calculations are

also described in Ref. 33.

Fig. 6 shows typical energy spectra for the H + Br_2 and Mu + Br_2 systems obtained from the Fourier transform of the calculated autocorrelation functions. Vertical dotted lines in Fig. 6 correspond to the vibrational energy levels of the asymptotic H(Mu) + Br_2(v, j = 0) reactants. In particular, for the H + Br_2 reaction system, many sharp resonances can be seen below and above the H + Br_2(v, j = 0) asymptotic levels. This is a clear evidence that these resonances are associated with the H···Br_2 van der Waals well. Of course, this assignment can easily be confirmed by looking at the wave packet evolution graphically. We have carried out the wave packet propagation with some different initial wave packet conditions (energy widths or initial locations), but found that the positions and widths of van der Waals resonances were not significantly sensitive to those initial conditions. In the case of the Mu + Br_2 reaction system, it is seen that resonances are less dense compared to the H + Br_2 system and that resonance widths become somewhat broader. This is also reasonable because of the mass difference between H and Mu. The most important point which should be discussed is to understand how these van der Waals resonances affect the overall H(Mu) + Br_2 reaction kinetics. From the cumulative reaction probabilities presented in Fig. 4, we can see that van der Waals resonances play some roles; however, it should be noted that thermal rate constants are quantities averaged over the collision energy due to the Boltzmann distribution. This suggests that, if the van der Waals resonance peaks are very sharp, such resonances are not so important for determining bimolecular rate constants. Nevertheless, we would like to point out that such van der Waals resonances may presumably play some roles under high-pressure conditions, where the third-body effect cannot be ignored. In fact, it should be emphasized that previous rate constant measurements [1, 2] for the H + Br_2 and Mu + Br_2 reactions have been carried out under relatively high pressure conditions. For example, the measurement for Mu + Br_2 were performed in 3 bar N_2 [1]. Although the importance of the van der Waals resonances have not been pointed out in any previous reports, we hope that the present theoretical study will stimulate further experimental studies. In particular, measurement of the pressure dependence of thermal rate constants would give important

information for understanding the reaction dynamics.

Finally, let us consider vibrational bonding for the Br-Mu-Br system on the present ab initio potential energy surface. As mentioned in Introduction, Ghandi et al. [15] have recently observed that a muoniated free radical is formed from the reaction of Mu with Br_2. Although its detailed structure was not confirmed, they have tentatively concluded that the observed radical has a nearly collinear Br-Mu-Br form, in which the Mu dynamical motion and the van der Waals attractive interaction between MuBr and Br prevent the dissociation of the Br-Mu-Br system in MuBr + Br. In order to confirm their assignment, they have further carried out purely classical dynamics calculations on the B3LYP/6-311G(2df, 2p)-level potential energy surface and confirmed the production of the Br-Mu-Br radical. However, since the dynamical vibrational bonding phenomenon in Br-Mu-Br is quantum-mechanical in nature, as mentioned in Introduction, the vibrational structures of Br-Mu-Br should be treated quantum-mechanically. In fact, Clary and Conner [17, 18] have previously performed such calculations but on less accurate semiempirical potential energy surfaces. Thus, it is quite interesting to perform three-dimensional bound-state calculations using the present ab initio potential energy surface. However, it should be emphasized that the present ab initio potential surface does not account for the effect of spin-orbit interaction as well as the electronically nonadiabatic effect. As mentioned before, since spin-orbit interaction should play a very important role in the Br + HBr asymptotic region, we have to point out that our quantum calculations presented below are only qualitative.

The bound-state calculations for the Br-Mu-Br system were done using the standard three-dimensional DVR approach [32] on the hyperspherical coordinates. The calculations were carried out only for $J = 0$. Numerical parameters were carefully chosen to obtain fully converged computational results. As a result, we have found that the Br-Mu-Br system has many vibrational states below the lowest Br + MuBr($v = j = 0$) asymptotic energy level on the present ab initio potential surface similar to the previous theoretical calculations by Clary and Connor [17, 18]. Fig. 7 shows contour plots of the calculated wave functions of the lowest two vibrational states of the

Br-Mu-Br system as a function of the Jacobi radical coordinates. It is seen that both wave functions are highly localized around the saddle point region but are not localized around the van der Waals regions. Thus, these plots clearly imply that these states have a feature of dynamical vibrational bonding typically seen for heavy-light-heavy reaction systems. Notice that the wave function of the second lowest state has a node along the asymmetric stretch coordinate. Only collinear configurations are presented in Fig. 7, but it should be mentioned that the maximum of the wave function density was observed around $\gamma \sim 140$-150 degrees, where γ is the Jacobi rotational angle. This is quite natural since the saddle point of the Br + HBr' $\rightarrow$ HBr + Br' exchange reaction occurs in a bent configuration as was presented in Fig. 3. It was also found that the energy levels of the lowest and second lowest vibrational states are 0.039 and 0.034 eV below the Br + MuBr($v = j = 0$) asymptotic energy level, respectively. This simply means that the vibrational bond energy for the lowest Br-Mu-Br state on the present ab initio potential surface is 0.039 eV. This value is much smaller than the previous theoretical value (0.13 eV) of Clary and Connor [18]. This is, however, not surprising since they have employed the semiempirical potential energy surface developed on the basis of the well-known diatomics-in-molecule (DIM) approach. In fact, the saddle point for the Br + HBr' $\rightarrow$ HBr + Br' exchange reaction on the DIM potential surface occurs at the collinear configuration and the corresponding barrier height is reported to be only 0.035 eV. We believe that our ab initio potential energy surface is much more realistic than the old DIM potential surface; however, we have to conclude that more quantitative treatments [27, 28] including the effect of nonadiabatic transitions induced by large spin-orbit interaction will definitely be necessary for obtaining accurate energy levels of the Br-Mu(H)-Br vibrational bonding molecule. Nevertheless, we would like to emphasize that the present theoretical calculations qualitatively support the experimental suggestion that the experimentally observed radical containing a Mu atom is the Br-Mu-Br vibrational bonding molecule. If this exotic molecule would be truly produced in the Mu + Br_2 reaction, it should be emphasized that a third body, that can carry away the large excess energy, also should play a very important role in the production dynamics. Therefore, understanding the three-body effect in the H(Mu) +

Br_2 reaction dynamics should be an important next step in the future theoretical studies and research along this line is currently underway in our laboratory.

4. Summary

In this work we have constructed a new global ab initio potential energy surface for the H + Br_2 → HBr + Br reaction at the MRCI+Q/aug-cc-pVTZ level of theory with a moderate accuracy. This ab initio level of theory was chosen after tests over some ab initio levels. We have found that the RCCSD(T) level calculations give a very small positive barrier just above the H + Br_2 reactant energy level while the MRCI+Q level calculations show that the barrier position is below the reactants.

We have performed time-independent quantum dynamics calculations to obtain the cumulative reaction probabilities for the H + Br_2 → HBr + Br and Mu + Br_2 → MuBr + Br reactions on the newly developed potential energy surface. It was found that the cumulative reaction probabilities for both reactions give a very similar behavior around the reaction threshold region. Although quantum dynamics calculations were done only for J = 0, this result is in disagreement with the previous rate constant measurements, where a positive activation energy was observed for H + Br_2 while a negative activation energy was obtained for Mu + Br_2. However, we have pointed out the importance of the van der Waals resonances associated with the entrance van der Waals well since the previous rate constant measurements were done under relatively high-pressure conditions.

Variational calculations of vibrational energy levels have been performed in order to study dynamical vibrational bonding of the Br-Mu-Br molecule on the developed ab initio potential energy surface. It was found that the system has several vibrational bonding states, whose wave functions are localized around the saddle point region of the Br + MuBr' → MuBr + Br' exchange reaction, below the lowest Br + MuBr(v = j = 0) asymptotic energy level. Although the present study does not include the effect of spin-orbit interaction nor the corresponding electronically nonadiabatic

effect, our calculations qualitatively support the recent experimental finding that the observed muoniated radical is the Br-Mu-Br vibrational bonding molecule presumably produced in the Mu + Br_2 reaction.

Acknowledgement

This work was supported by the Grant-in-Aid for Scientific Research of the Ministry of Education, Culture, Sports, Science, and Technology of Japan (Grant No. 17550007).

References

[1] A. C. Gonzalez, I. D. Reid, D. M. Garner, M. Senba, D. G. Fleming, D. J. Arseneau, J. R. Kempton, J. Chem. Phys 91 (1989) 6164.

[2] Y. Wada, T. Takayanagi, H. Umemoto, S. Tsunashima, S. Sato, J. Chem. Phys. 94 (1990) 4896.

[3] P. W. Seakins, M. J. Pilling, J. Phys. Chem. 95 (1991) 9878.

[4] X. Giménez, J. M. Lucas, A. Aguilar, A. Laganà, J. Phys. Chem. 97 (1993) 8578.

[5] T. Takayanagi, Y. Kurosaki, J. Phys. Chem. A 101 (1997) 7089.

[6] M. González, J. Hijazo, J.J. Novoa, R. Sayós, J. Chem. Phys. 108 (1998) 3168.

[7] W. Jakubetz, J.N.L. Connor, P.J. Kuntz, Phys. Chem. Chem. Phys. 1 (1999) 1213.

[8] M. Bittererová, S. Biskupič, Chem. Phys. Lett. 299 (1999) 145.

[9] M. Bittererová, S. Biskupič, H. Lischka, W. Jakubetz, Phys. Chem. Chem. Phys. 2 (2000) 513.

[10] J. Han, M. C. Heaven, G. C. Manke II, J. Phys. Chem. A 106 (2002) 8417.

[11] O. Dobis, S. W. Benson, J. Phys, Chem. A 106 (2002) 4403.

[12] H. Wang, X, Sun, D. Feng, Z. Cai, J. Theo. Comp. Chem. 5 (2006) 307.

[13] J. W. Hepburn, D. Klimek, , K. Liu, J. C. Polanyi, S. C. Wallace, J. Chem. Phys. 69 (1978) 4311.

[14] J. D. McDonald, P. R. LeBreton, Y. T. Lee, D. R. Herschbach, J. Chem. Phys. 56 (1972) 769.

[15] K. Ghandi K, S. P. Cottrell SP, D. G. Fleming, C. Johnson C, Physica B (Condensed Matter) 374 (2006) 303.

[16] J. Manz, R. Meyer, E.. Pollak, J. Römelt, Chem. Phys. Lett. 93 (1981) 184.

[17] D. C. Clary, J. N. L. Connor, Chem. Phys. Lett. 94 (1983) 81.

[18] D. C. Clary, J. N. L. Connor, J. Phys. Chem. 88 (1984) 2758.

[19] R. B. Metz, A. Weaver, S. E. Bradforth, T. N. Kitsopoulos, D. M. Neumark. J. Phys. Chem. 94 (1990) 1377.

[20] S. R. Langhoff, E. R. Davidson, Int. J. Quantum Chem. 8 (1974) 61.

[21] E.R. Davidson, J. Comp. Chem. 17 (1975) 87.

[22] T. H. Dunning, Jr., J. Chem. Phys. 90 (1989) 1007.

[23] R. A. Kendall, T. H. Dunning, Jr., R. H. Harrison, J. Chem. Phys. 96 (1992) 6796.

[24] H.-J. Werner, P. J. Knowles, J. Chem. Phys. 82 (1985) 5053.

[25] P. J. Knowles, H.-J. Werner, Chem. Phys. Lett. 115 (1985) 259.

[26] MOLPRO, a package of ab initio programs, H.-J. Werner and P. J. Knowles, version 2002.1, R. D. Amos, A. Bernhardsson, A. Berning, P. Celani, D. L. Cooper, M. J. O. Deegan, A. J. Dobbyn, F. Eckert, C. Hampel, G. Hetzer, P. J. Knowles, T. Korona, R. Lindh, A. W. Lloyd, S. J. McNicholas, F. R. Manby, W. Meyer, M. E. Mura, A. Nicklass, P. Palmieri, R. Pitzer, G. Rauhut, M. Schütz, U. Schumann, H. Stoll, A. J. Stone, R. Tarroni, T. Thorsteinsson, and H.-J. Werner.

[27] M. Hankel, J. N. L. Connor, G. C. Schatz. Chem. Phys. 308 (2005) 225.

[28] M. Meuwly, J. M. Hutson, Phys. Chem. Chem. Phys. 2 (2000) 441.

[29] D. Skouteris, J. F. Castillo, D. E. Manolopoulos, Comp. Phys. Comm. 133 (2000) 128.

[30] T. Takayanagi, Y. Kurosaki, J. Chem. Phys. 109 (1998) 8929.

[31] R. T Pack, G.A. Parker, J. Chem. Phys. 87 (1987) 3888.

[32] J. C. Light, I. P. Hamilton, J. V. Lill, J. Chem. Phys. 82 (1985) 1400.

[33] T. Takayanagi, A. Wada, Chem. Phys. Lett. 352 (2002) 91.

Figure Captions

Fig. 1 One-dimensional potential energy profiles as a function of the H-Br distance.

Fig. 2 Two-dimensional contour plots of the potential energy surface for the H + Br_2 $\rightarrow$ HBr + Br reaction as a function of *R*(H-Br) and R(Br-Br) distances for several values of $\angle$H-Br-Br angle. Zero of the energy is taken to be the reactant H + Br_2 potential minimum. Contours are spaced by 0.1 eV; solid curves are used for energies that are positive relative to H + Br_2, dashed curves are used for energies which are negative, and bold lines denote the zero contours.

Fig. 3 Two-dimensional contour plots of the potential energy surface for the Br + HBr' $\rightarrow$ HBr + Br' exchange reaction as a function of *R*(H-Br) and R(H-Br') distances for several values of $\angle$Br-H- Br' angle. Plot conventions are the same as Fig. 2.

Fig. 4 Cumulative reaction probabilities as a function of the total energy for the H + Br_2 $\rightarrow$ HBr + Br (a) and Mu + Br_2 $\rightarrow$ HBr + Br (b) reactions. Plot inserts are expansions of cumulative reaction probabilities around the reaction threshold region. Vertical dotted lines correspond to reactant energy levels of H(Mu) + Br_2(v, j)

Fig. 5 Schematic decay mechanism of the resonance associated with the H(Mu)$\cdots$$Br_2$ van der Waals well.

Fig. 6 Energy spectra obtained from the autocorrelation functions calculated by time-dependent wave packet evolutions. Vertical dotted lines show the energy levels of the H(Mu) + Br_2(v = 0, 1, 2, 3 and 4, j = 0) reactants.

Fig. 7 Contour plots of wave functions of the lowest two vibrational states for the Br-Mu-Br system as a function of Jacobi radical coordinates in collinear configurations:

the lowest state (a) and the second lowest state (b). Positive and negative contours are shown as solid and dashed lines, respectively. A node is clearly seen in the contour plot of the wave function for the second lowest state.

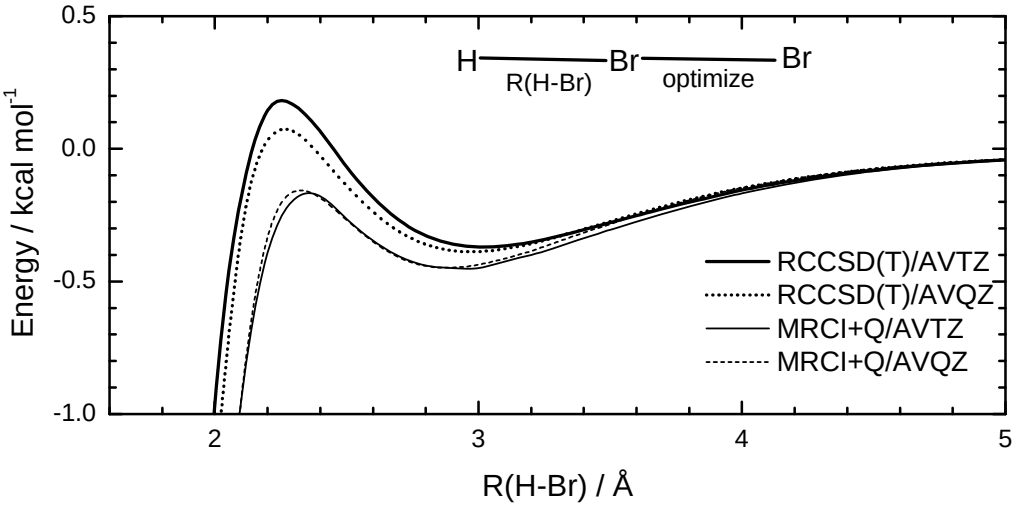
0.5
0.0
-0.5
-1.0
Energy / kcal mol-1
2
3
4
5
R(H-Br) / Å
H
Br
Br
R(H-Br)
optimize
RCCSD(T)/AVTZ
RCCSD(T)/AVQZ
MRCI+Q/AVTZ
MRCI+Q/AVQZ

Figure 1

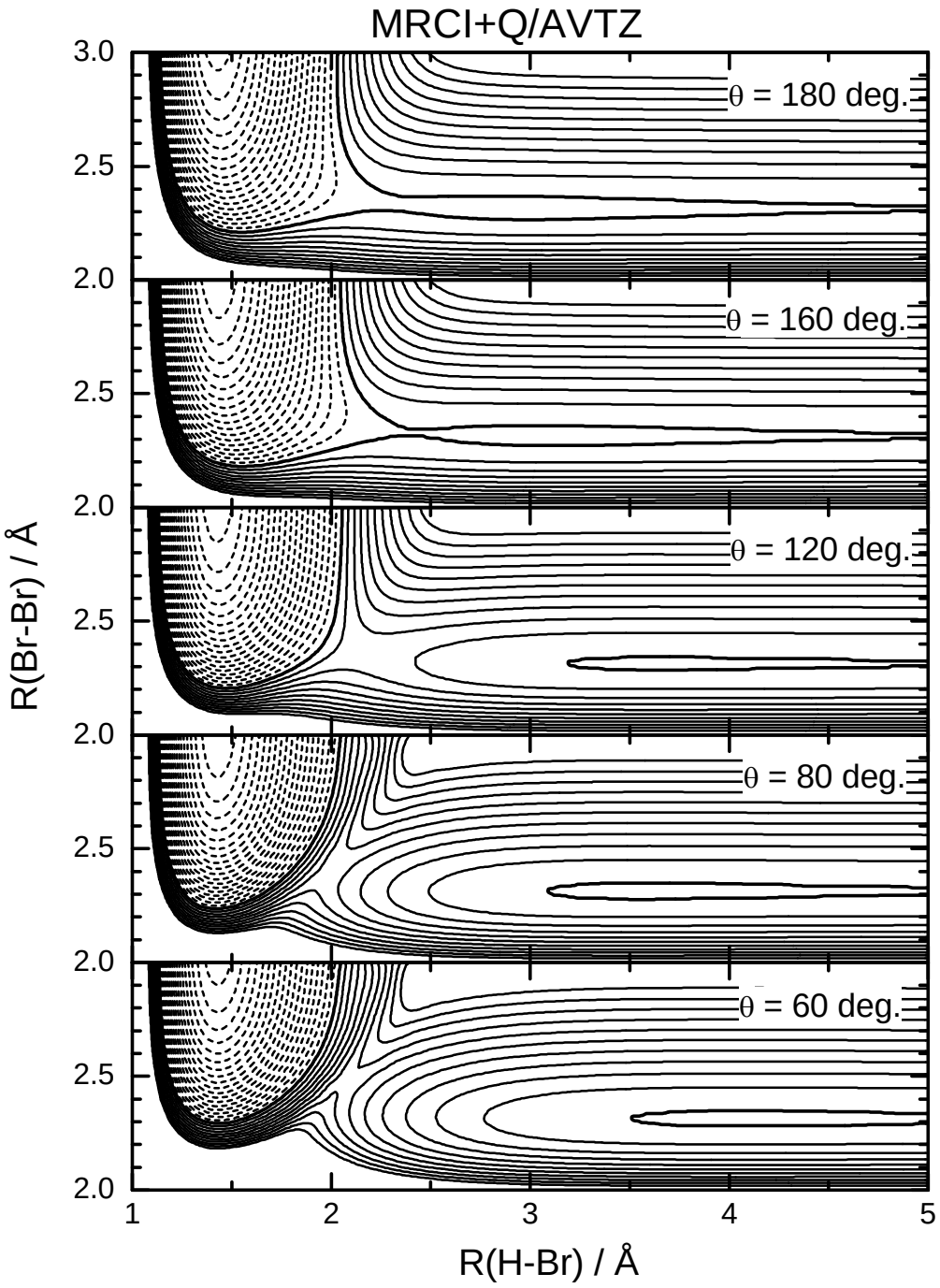
MRCI+Q/AVTZ
θ = 180 deg.
θ = 160 deg.
θ = 120 deg.
θ = 80 deg.
θ = 60 deg.
R(Br-Br) / Å
R(H-Br) / Å
3.0
2.5
2.0
1
2
3
4
5

Figure 2

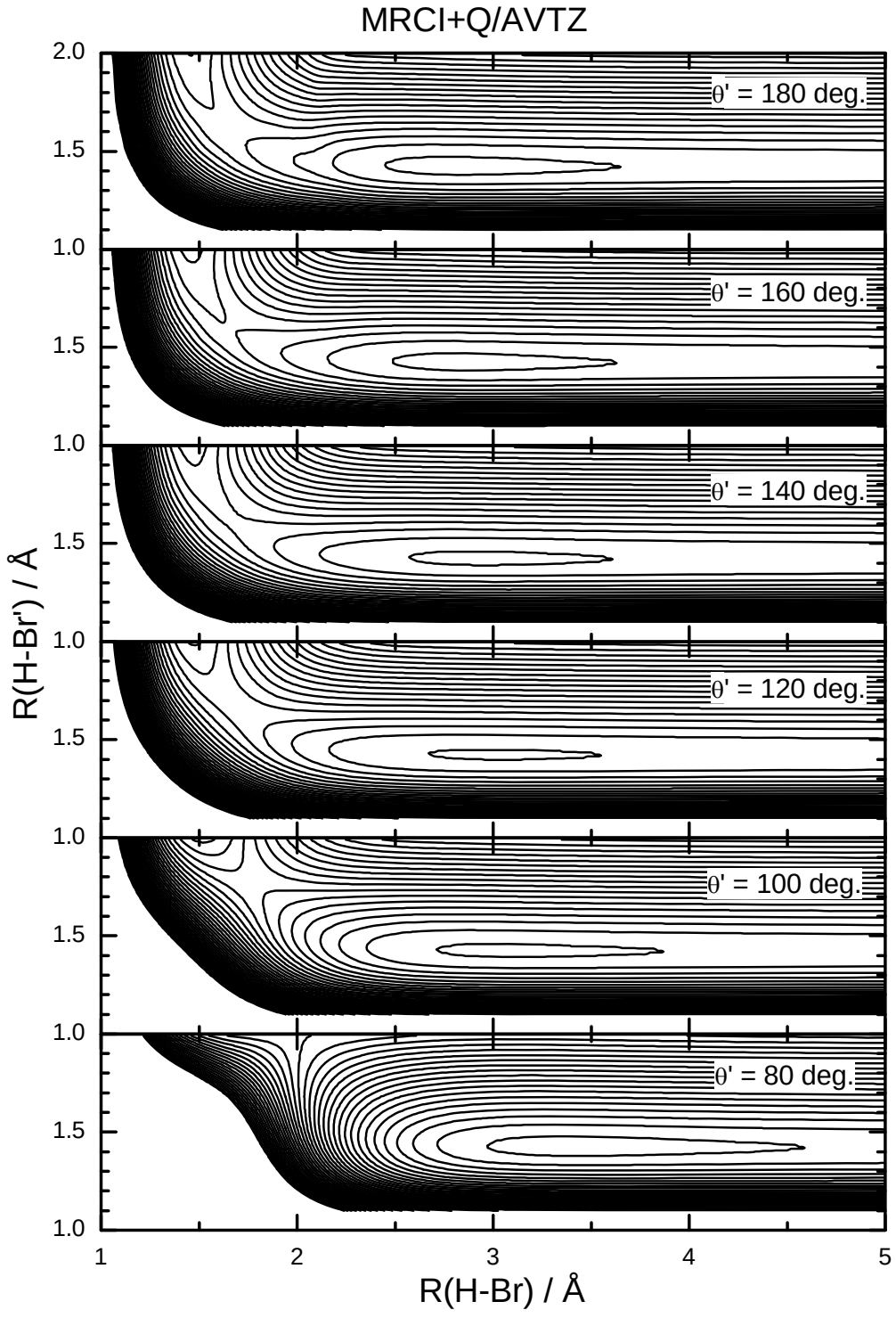
MRCI+Q/AVTZ
θ' = 180 deg.
θ' = 160 deg.
θ' = 140 deg.
θ' = 120 deg.
θ' = 100 deg.
θ' = 80 deg.
R(H-Br') / Å
R(H-Br) / Å
2.0
1.5
1.0
1
2
3
4
5

Figure 3

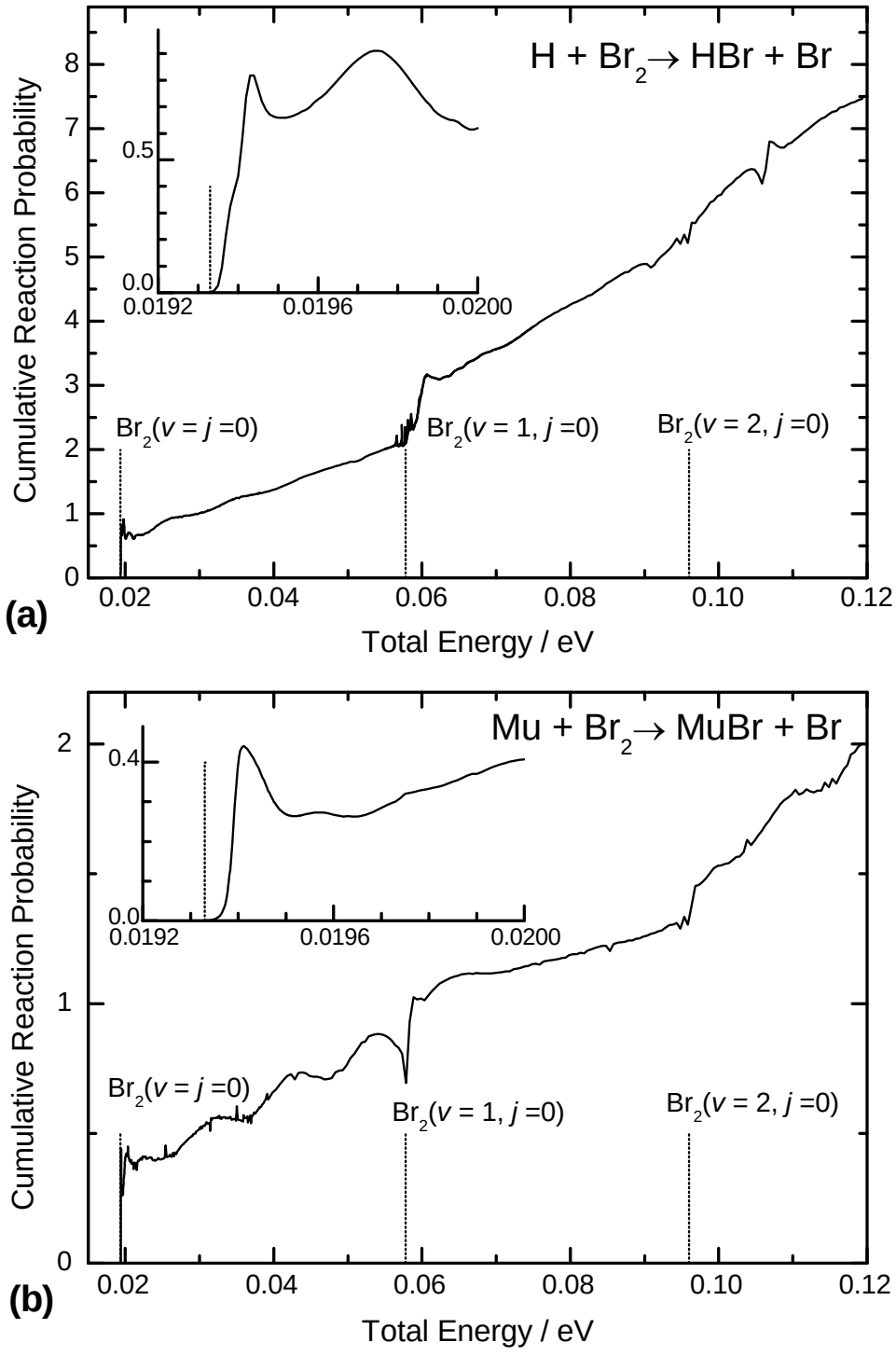
H + Br2 → HBr + Br
Cumulative Reaction Probability
Total Energy / eV
Br2(v = j =0)
Br2(v = 1, j =0)
Br2(v = 2, j =0)
(a)
Mu + Br2 → MuBr + Br
Cumulative Reaction Probability
Total Energy / eV
Br2(v = j =0)
Br2(v = 1, j =0)
Br2(v = 2, j =0)
(b)

Figure 4

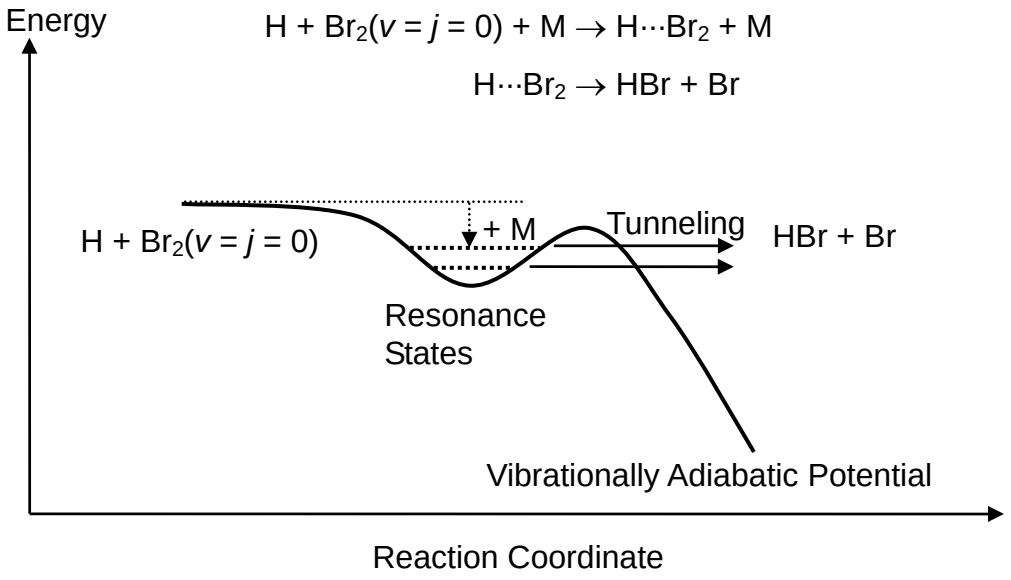
Energy
H + Br2(v = j = 0) + M → H···Br2 + M
H···Br2 → HBr + Br
H + Br2(v = j = 0)
+ M
Tunneling
HBr + Br
Resonance
States
Vibrationally Adiabatic Potential
Reaction Coordinate

Figure 5

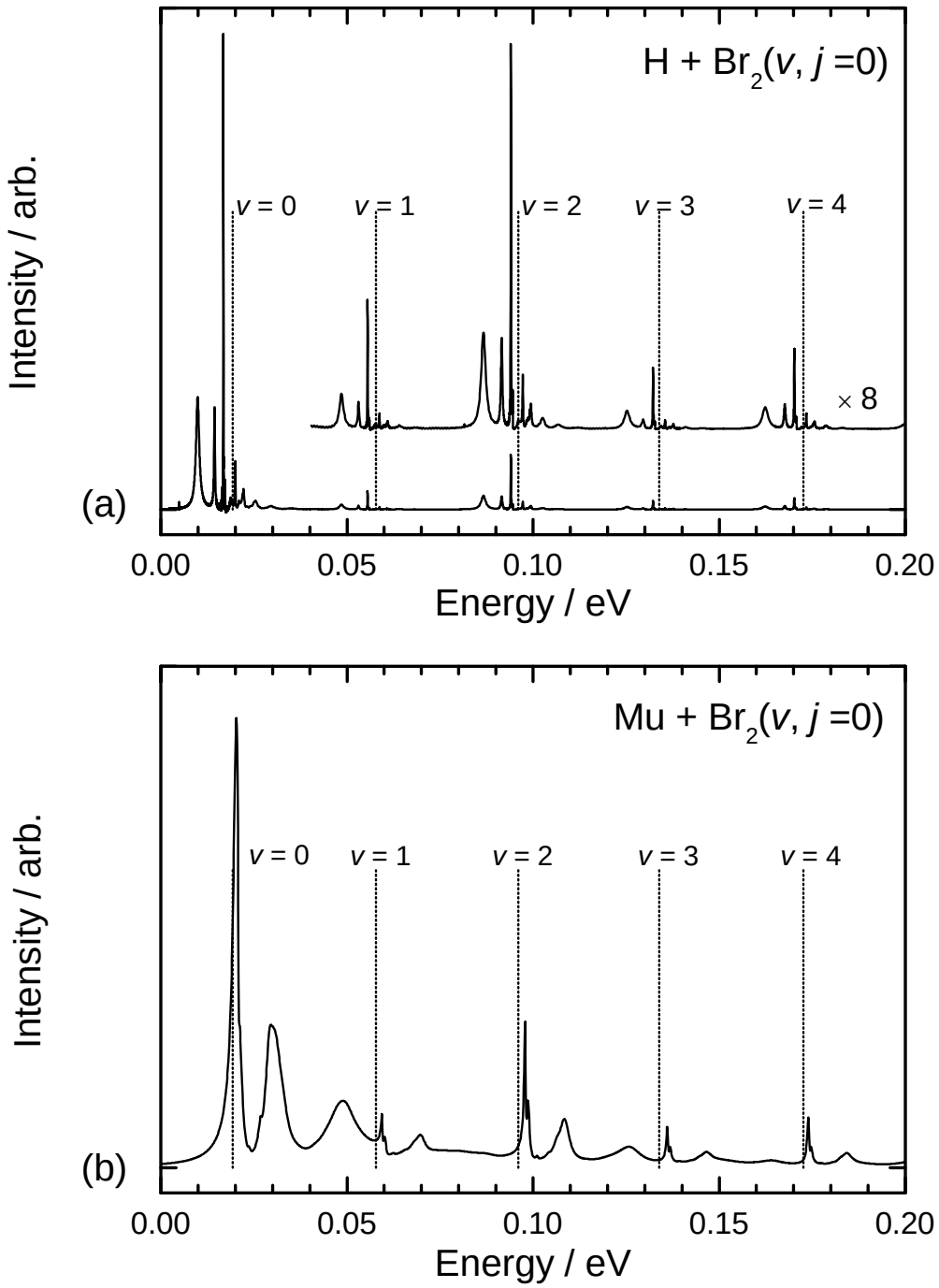
H + Br2(v, j =0)
v = 0
v = 1
v = 2
v = 3
v = 4
× 8
(a)
Intensity / arb.
0.00
0.05
0.10
0.15
0.20
Energy / eV
Mu + Br2(v, j =0)
v = 0
v = 1
v = 2
v = 3
v = 4
(b)
Intensity / arb.
0.00
0.05
0.10
0.15
0.20
Energy / eV

Figure 6

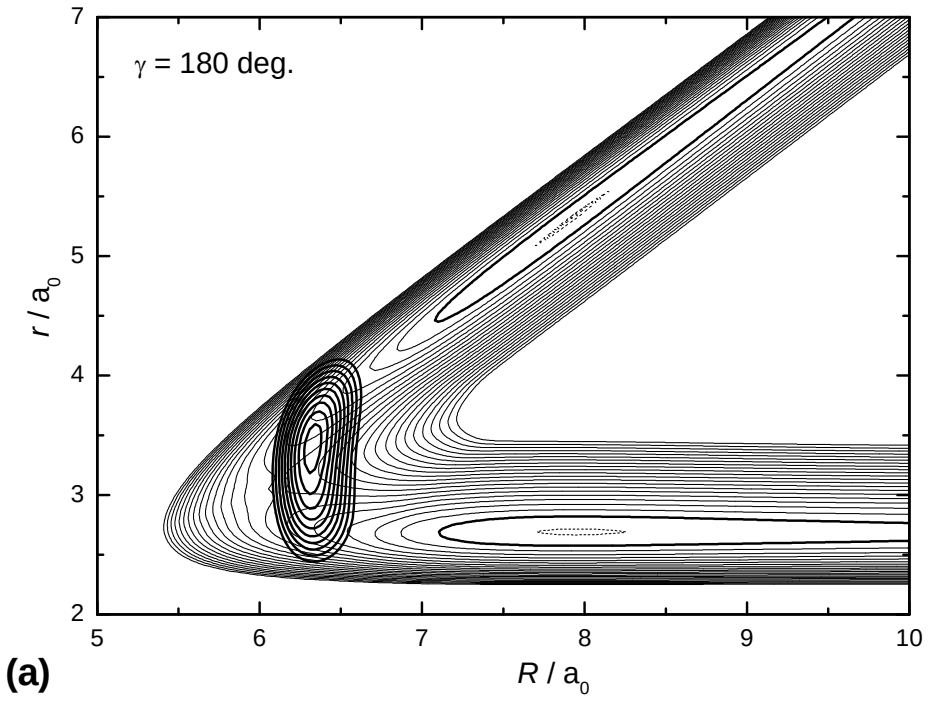

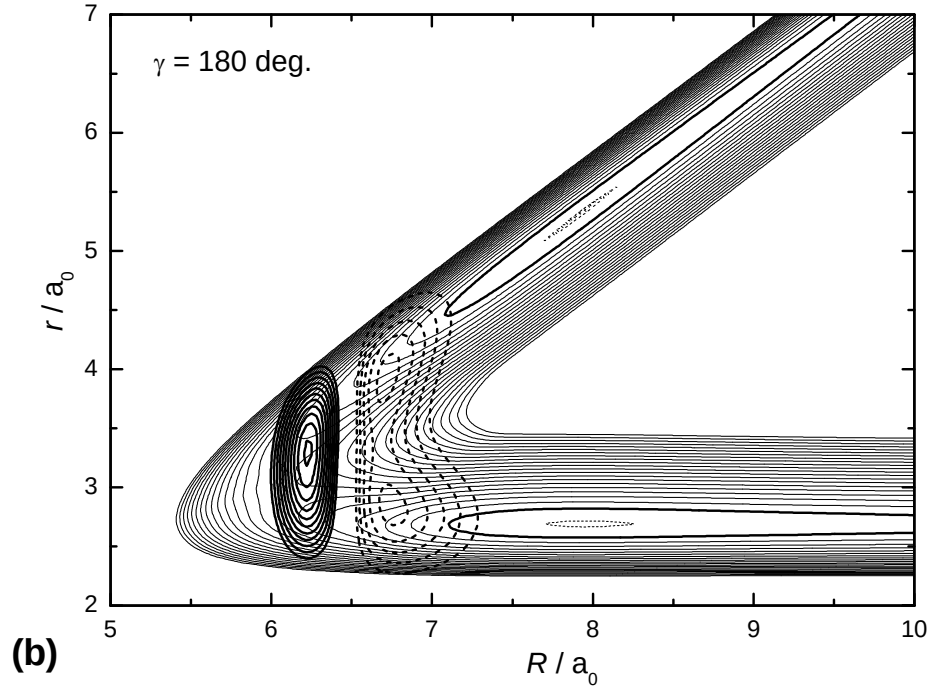

Figure 7